Alterations of cellular organelles in human liver-derived hepatoma G2 cells induced by adriamycin

Haoran Qian[a] and Yi Yang[b]

Adriamycin (ADM) is a commonly used chemotherapeutic drug in the treatment of hepatocellular carcinoma. However, the mechanisms involved in ADM-induced cell death and the molecular basis of ADM resistance are still unclear. To observe the early events that occurred in hepatoma cells in response to ADM, we investigated the alterations of morphology and subcellular distributions of cellular organelles in human liver-derived hepatoma G2 (HepG2) cells after ADM treatment. HepG2 cells were exposed to different doses of ADM for up to 60 h. Cytotoxicity occurred 24 h after 0.05 μg/ml ADM application, and remaining living cells showed irregular shapes but continued to multiply. Some cellular organelles altered their subcellular distribution or morphology after ADM treatment, including mitochondria, autophagic vacuoles, and Golgi apparatus. Immunoblotting with anti-LC3 antibody showed the upregulation of LC3-II protein, confirming that ADM leads to the induction of autophagy in HepG2 cells. Our findings suggest that among most of the cellular organelles, mitochondria and autophagic vacuoles were involved in the early ADM response, and may contribute to ADM-induced HepG2 cell death. ***Anti-Cancer Drugs*** **20:779–786 © 2009 Wolters Kluwer Health | Lippincott Williams & Wilkins.**

Anti-Cancer Drugs 2009, **20**:779–786

Keywords: adriamycin (doxorubicin), autophagy, hepatoma G2 cells, mitochondria

[a]Department of General Surgery, Institute of Micro-Invasive Surgery of Zhejiang University, Sir Run Run Shaw Hospital, Medical College of Zhejiang University and [b]Department of Biomedical Engineering, Key Laboratory of Biomedical Engineering of Ministry of Education, Zhejiang University, Hangzhou, PR China

Correspondence to Dr Haoran Qian, MD, Department of General Surgery, Sir Run Run Shaw Hospital, Medical College of Zhejiang University, Hangzhou, 310016, PR China
Tel: +86 571 86090073; e-mail: websterqian@hotmail.com

Received 5 March 2009 **Accepted** 10 June 2009

Introduction

Hepatocellular carcinoma (HCC) is one of the most common types of fatal cancer and arises from multiple risk factors in humans. Adriamycin (ADM, also called doxorubicin) is a cytotoxic anthracycline antibiotic isolated from cultures of *Streptomyces peuxetus*, and has been widely used as the anticancer drug in the treatment of HCC [1,2]. The underlying mechanism is related to its potential role of DNA synthesis inhibition, free radical formation and lipid peroxidation, DNA binding and alkylation, DNA cross-linking, interference with DNA strand separation and helicase activity, direct membrane effects, and the initiation of DNA damage through the inhibition of topoisomerase II in tumor cells [3]. However, development of resistance to chemotherapy drugs is a major obstacle in clinical oncology and might be particularly involved in the consequent chemotherapy failure frequently observed in HCC [4–6]. The process leading to killing of cancer cells and the molecular basis of resistance to ADM are still unclear.

ADM has been shown to induce rapid cell shrinkage, increase cell granularity, chromatin condensation, and mitochondrial membrane potential collapse in human liver-derived hepatoma G2 (HepG2) cells [7]. It also regulated endoplasmic reticulum (ER) stress-induced apoptosis by disrupting the unfolded protein response in human breast carcinoma cells [8]. The well-known drug resistance marker P-glycoprotein (P-gp) has been found to be located in the Golgi apparatus in ADM-induced resistant cells [9]. These raise a question as to which specific cellular organelle is the target of ADM-induced cell death.

We herein investigated the alteration of cellular organelles including mitochondria, ER, Golgi apparatus, autophagic vacuoles (AVs), and lysosomes in HepG2 cells induced by ADM.

Methods

Materials

All reagents were purchased from Sigma-Aldrich (St. Louis, Missouri, USA) except those specifically mentioned.

Cell culture and ADM treatment

Human hepatoma cell line HepG2 and human normal hepatocyte LO2 were purchased from Chinese Academy of Sciences (Shanghai, China). Cells were routinely cultured in Dulbecco's modified Eagle's medium (DMEM; GIBCO BRL, Grand Island, New York, USA), supplemented with 10% fetal bovine serum, penicillin (100 U/ml), streptomycin (0.1 mg/ml), and were maintained

0959-4973 © 2009 Wolters Kluwer Health | Lippincott Williams & Wilkins DOI: 10.1097/CAD.0b013e32832f4e6f

in a humidified atmosphere of 5% CO_2 at 37°C. Cells were passaged every 4–5 days. For ADM treatment, appropriate amounts of stock solution (2.5 mmol/l in dimethyl sulfoxide) of ADM (Pharmacia, Peapack, New Jersey, USA) were added to culture medium to achieve the indicated concentrations. To evaluate cell proliferation, cells were incubated with 0, 0.01, 0.05, or 0.1 μg/ml of ADM for up to 60 h before they were subjected to MTT, 3-(4,5-dimethylthiazol-2-yl)-2,5-diphenyltetrazolium bromide, assay. For western blotting, cells were treated with 0.05 μg/ml ADM for up to 60 h before protein extraction. In each experiment, culture medium was changed and ADM was re-added every 24 h. Other experiments were carried out after a 24-h treatment with 0.05 μg/ml ADM.

Hoechst 33342 staining

After treatment with ADM, cells were fixed with 4% paraformaldehyde for 15 min at room temperature, then washed three times with phosphate buffered saline (PBS) and exposed to 10 mg/l Hoechst 33342 at 37°C in the dark for 15 min. After washing three times with PBS, samples were observed under fluorescence microscopy (X71; Olympus, Tokyo, Japan). The number of apoptotic cells was counted per area and was presented as a percentage of the total number of cells. At least 15 photomicrographs were evaluated randomly per treatment and each treatment was performed in triplicate.

Determination of cell proliferation

To evaluate the cell proliferation, the MTT assay was performed. Each data point represented results from three independent experiments and each treatment was performed in sextuplicate. Cells were seeded into 96-well plates at a density of 500 cells/well. On the next day, cells were incubated with different concentrations of ADM. After the appropriate incubation time, 15% volume of MTT (5 mg/ml) was added to each well. After another 4 h of incubation at 37°C, the medium was removed and 100 μl dimethyl sulfoxide was added to each well to resuspend the MTT metabolic product. The absorbance of the dissolved formazan was measured at 570 nm (A_{570}) with a microplate reader (Versa Max; Molecular Devices, California, USA). The percentage of cell proliferation was calculated by the formula:

$$\text{Cell proliferation}\ (\%) = 100 - [(A_{570,\text{Control}} - A_{570,\text{ADM}})/A_{570,\text{Control}}] \times 100$$

Transmission electron microscopy analysis

The cells were harvested by trypsinization, washed twice with PBS, and fixed in 0.1 mol/l sodium cacodylate-buffered (pH 7.4) 2.5% glutaraldehyde solution for 2 h and postfixed in 0.1 mol/l sodium cacodylate-buffered (pH 7.4) 1% osmium tetroxide solution for 1 h. After dehydration in an ethanol gradient [70% (v/v) ethanol (15 min), 80% (v/v) ethanol (15 min), 90% (v/v) ethanol (15 min), 100% ethanol (2×20 min)], samples were incubated with propylenoxide (2×10 min), impregnated with a mixture of propylenoid/LX-112 (1 : 1; Ladd Research Industries, Williston, Vermont, USA) and embedded in LX-112. Ultrathin sections were stained with uranyl acetate and lead citrate. Sections were examined in a Jeol-100 CX II transmission electron microscopy (TEM) at 80 kV.

Transfection

Transient transfection with DsRed-Mit plasmid (Clontech, Mountain View, California, USA), GFP-KDEL plasmid (kindly provided by B. Boyles), Golgi-GFP plasmid (kindly provided by D. Toomre), ptdTomato-LC3 plasmid (kindly provided by Dr T. Johansen), GFP-Lgp120 plasmid (kindly provided by Dr P. Luzio), or GFP-α-tubulin plasmid (Clontech) was carried out as described earlier [10]. Briefly, Lipofectamine 2000 (Invitrogen, California, USA) transfection reagent was used for transfection 1 day after subculture. For each well in a 24-well plate, 1 μg DNA in 25 μl DMEM was combined with 2 μl Lipofectamine 2000 in 25 μl DMEM. Twenty minutes after incubation at room temperature, another 200 μl DMEM was added into the mixture. The cultures were left for 4 h in this transfection medium, and then it was replaced by fresh culture medium. Transfection efficiency was about 80% under this condition.

Immunoblotting

Proteins were extracted from HepG2 cells using radioimmunoprecipitation assay buffer. Protein extracts were separated on SDS–polyacrylamide gel, transferred to a polyvinylidene difluoride (PVDF) membrane (Millipore, Burlington, Massachusetts, USA), blocked with 5% skim milk in Tris-buffered saline containing 0.1% Tween (TBS-T), and then probed with anti-MAP LC3 (1 : 200; Santa Cruz Biotechnology, California, USA) at 4°C overnight. Secondary horseradish peroxidase-conjugated anti-rabbit IgG was used at a dilution of 1 : 2000 for 1 h at room temperature. Visualization of immunoreactive bands was performed with an enhanced chemoluminescence detection kit (Amersham Biosciences, Piscataway, New Jersey, USA). The same membrane was stripped and reprobed with anti-actin (1 : 2000; Santa Cruz Biotechnology) antibody for normalization. Western blot analysis was performed in triplicate.

Statistical analysis

The data were plotted as mean ± SD from three independent experiments. Statistical significant differences were carried out by one-way analysis of variance followed by Tukey's post-hoc tests. A P value of less than 0.001 was considered statistically significant.

Results

Cytotoxic effects of ADM on HepG2 cells

The cytotoxicity of ADM was determined by treating HepG2 cells with ADM at various concentrations for 12–60 h followed by the MTT assay. As ADM has a relatively short half-life, culture medium was changed and ADM was re-added every 24 h. The addition of ADM exerted a cytotoxic effect during the first 24 h incubation, as a significant decrease in cell proliferation occurred; thereafter a gradual increase was observed (Fig. 1a). For 0.1 μg/ml ADM application, increased proliferation was detected after 36 h. Optimal dosing of chemotherapeutic agents is critical not only for suppression of tumor growth, but also to minimize their cytotoxicity in normal cells. Therefore, we chose 0.05 μg/ml ADM and 24 h incubation time for the following experiments. Phase-contrast photomicrographs showed the differences in cell morphology between the ADM-treated group and control. Twenty-four hours after ADM treatment, some of the HepG2 cells died (Fig. 1b, upper panels, arrowheads), other living cells obviously showed a differentiation characteristic with long spines (Fig. 1b, upper panels, asterisks). Fluorescence microscopy of fixed HepG2 cells stained with Hoechst 33342 was used to enumerate cells with chromatin condensation patterns typical of apoptosis. Apoptotic cells with brightly stained nuclei and condensed chromatin could be detected at 24 h after ADM treatment (Fig. 1b, bottom panels, arrowheads) compared with untreated normal cells (Fig. 1b, bottom panels, arrows), and were further expressed as a percentage of total cell number (Fig. 1c). It should be noted that after removal of dead cells by medium replacement, the remaining cells were not only survived but also multiplied (data not shown).

ADM had no detectable effect on normal hepatocyte cells

To determine whether or not ADM has the damage effect on human normal hepatocyte cells, LO2 cells were used. Phase-contrast microphotographs showed no morphological difference between ADM-treated cells and control cells (Fig. 2a). Furthermore, almost no apoptotic LO2 cells could be observed after 24 h of ADM treatment (Fig. 2a and b) analyzed by Hoechst 33342 staining. After 24 h incubation with 0.05 μg/ml ADM, cells showed no significant difference in cell proliferation and viability as determined by the MTT assay (Fig. 2c).

Ultrastructures of HepG2 cells after ADM treatment

The ultrastructures of HepG2 cells, including membrane of nucleus, mitochondria, ER, and AVs, were investigated under TEM. After 24 h of ADM (0.05 μg/ml) treatment, most of the principal cellular organelles were not distinctly different from those of control cells (Fig. 3). The membrane of nucleus was normal in appearance. There was no obvious difference in the morphology of ER at this time point (Fig. 3a a3 and Fig. 3b b3,

Fig. 1

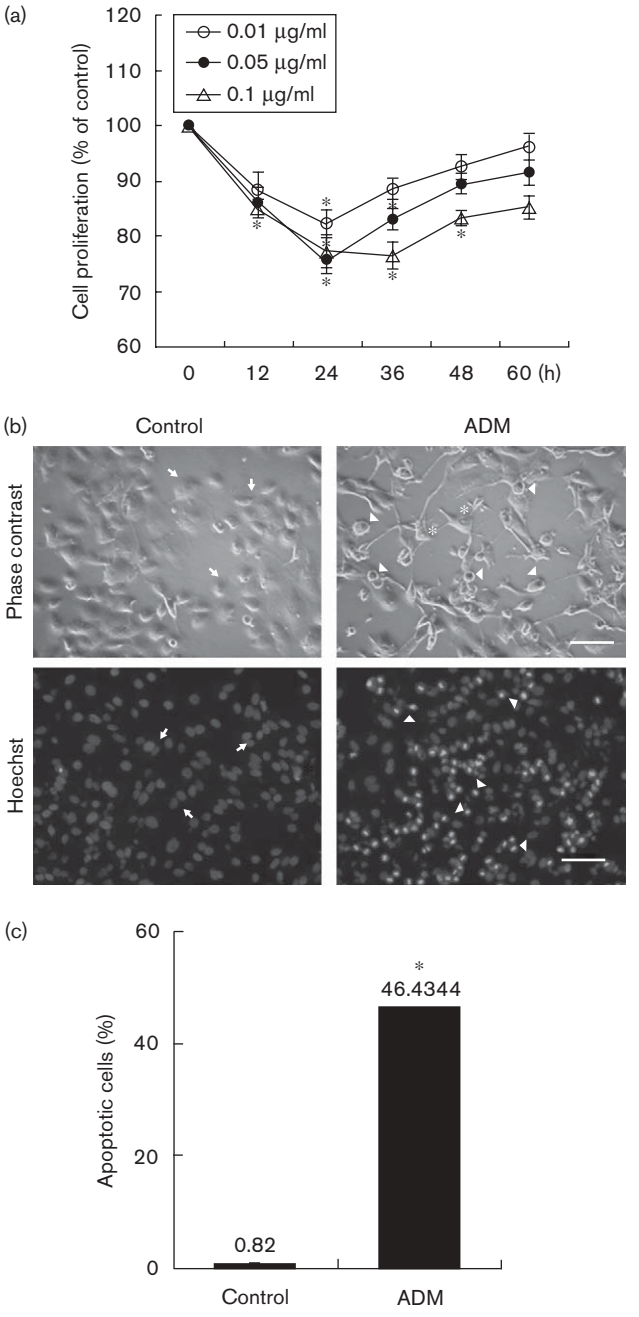

Cytotoxic effects of adriamycin (ADM) on human liver-derived hepatoma G2 (HepG2) cells. (a) Effect of ADM on the viability of HepG2 cells. Cells were treated with 0, 0.01, 0.05, or 0.1 μg/ml of ADM for 12, 24, 36, 48, or 60 h before they were subjected to an MTT assay for cell viability. The data were presented as percentage of the control (dose 0) and were plotted as mean ± SD from three independent experiments. *$P < 0.001$ compared with control (0 h). (b) Apoptotic cell death induced by ADM in HepG2 cells. Representative phase-contrast images were taken 24 h after 0.05 μg/ml ADM treatment (upper panels). Arrows: normal cells; arrowheads: dead cells; asterisks: cells with irregular shapes. Hoechst 33342 was used to assess the cell apoptosis (bottom panels). Arrows: normal cells; arrowheads: cells with condensed chromatin. Scale bars: 100 μm. (c) Quantification of apoptotic cell death induced by ADM. *$P < 0.001$ compared with untreated control.

Fig. 2

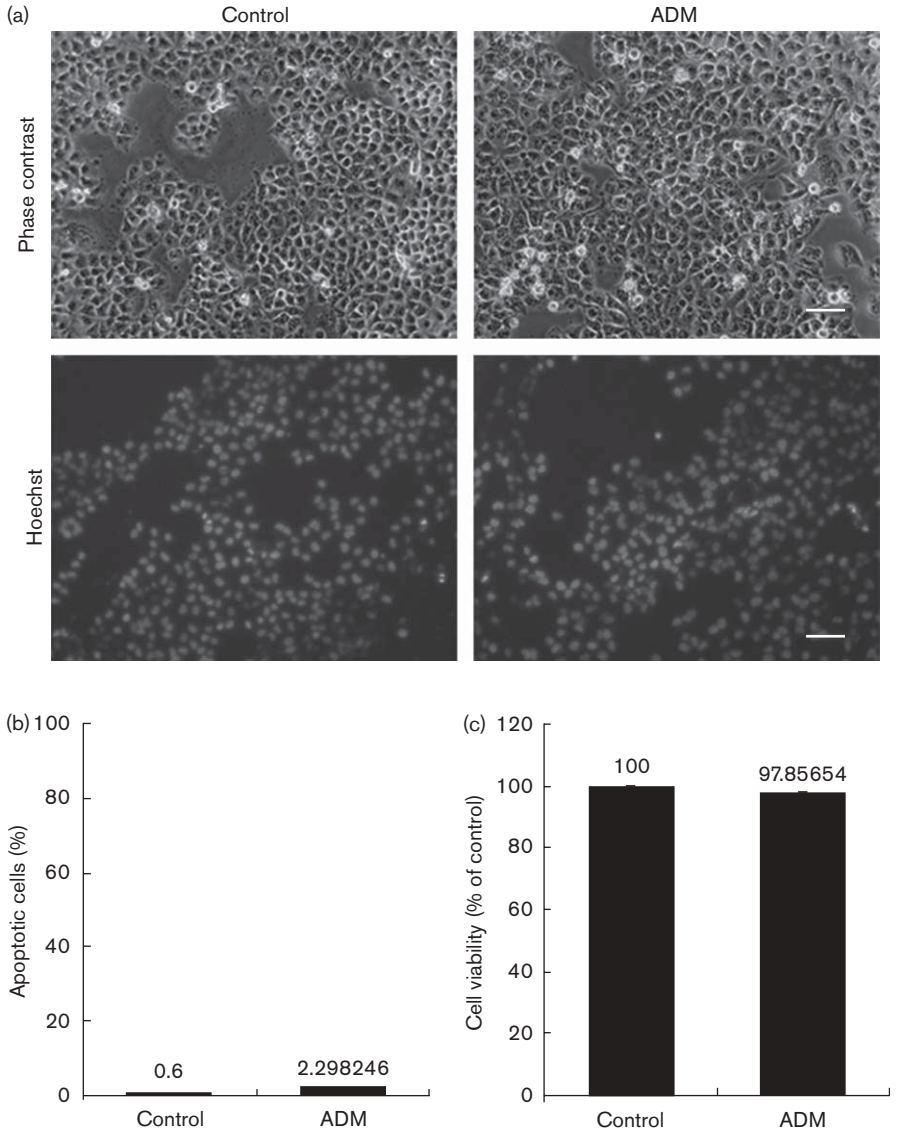

Effects of adriamycin (ADM) on LO2 cells. (a) ADM did not induce cell apoptosis in LO2 cells. Representative phase-contrast images were taken 24 h after 0.05 μg/ml ADM treatment (upper panels). Hoechst 33342 was used to assess the cell apoptosis (bottom panels). Scale bars: 100 μm. (b) Quantification of apoptotic cell death induced by ADM. (c) Effect of ADM on the viability of HepG2 cells. Cells were treated with 0 or 0.05 μg/ml of ADM for 24 h before they were subjected to MTT assay for cell viability. The data were presented as a percentage of the control and were plotted as mean ± SD from three independent experiments.

arrowheads). Mitochondria in control cells were rod-like and elongated in shape. The matrix was fairly dark and uniform and the cristae were regularly distributed (Fig. 3a a1, a2, arrows). However, after ADM treatment, most of the mitochondria became small round structures with few, if any remaining, cristae (Fig. 3b b1, b2, arrows). Interestingly, numerous large cytoplasmic inclusions that were membrane-bound vacuoles characteristic of autophagy (termed AVs, double arrows) and autolysosomes (asterisks) occurred in the cells with ADM treatment (Fig. 3b b4), implying the induction of autophagic process.

Altered cellular organelles induced by ADM treatment

According to electron microscopy analysis, among all the organelles, mitochondria could be the first to be attacked by ADM treatment, and autophagic process is likely to be activated at 24 h after such treatment. To confirm this hypothesis, cellular organelles were labeled with different plasmids tagged with fluorescent proteins, respectively, by transfections. The morphology of mitochondria in HepG2 cells was determined by visualizing the distribution of transiently expressed DsRed-Mit. In control cells, long, branched or interconnected mitochondria, which were classified here as reticular, presented

Fig. 3

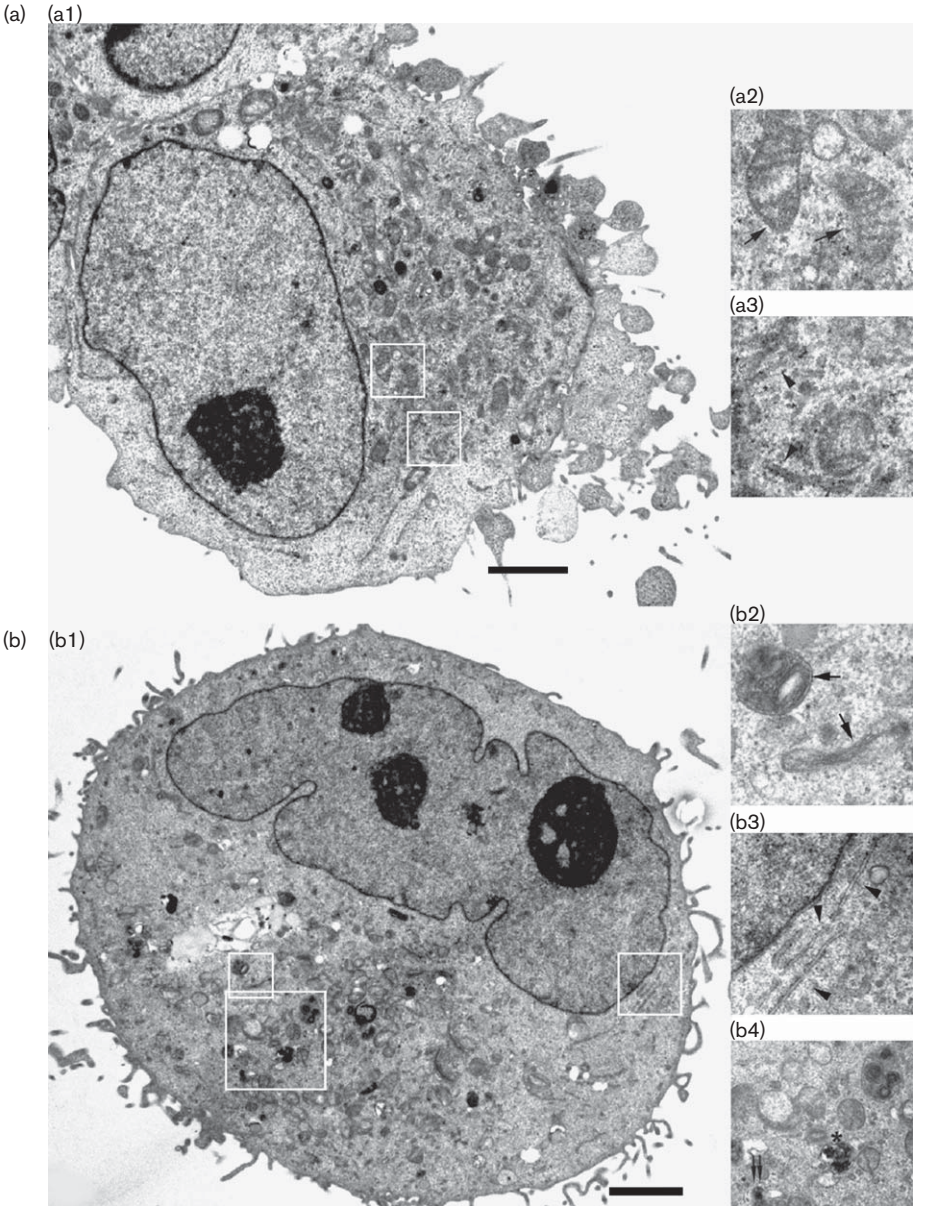

Ultrastructure of human liver-derived hepatoma G2 (HepG2) cells showed by transmission electron microscopy. (a) Control cells with intact nuclear membranes, mitochondria, and endoplasmic reticulum (ER). (a2) and (a3) are the enlarged images of (a1). Arrows: mitochondria; arrowheads: ER. (b) Cells after 0.05 μg/ml ADM treated for 24 h. (b2–b4) are the enlarged images of (b1). Arrows: mitochondria; arrowheads: ER; double arrows: autophagic vacuoles; asterisks: autolysosome. Scale bars: 2 μm.

throughout the cytoplasm (Fig. 4 a1). After ADM treatment, fragmented mitochondria, which were short, round or occasionally aggregated, were appeared in HepG2 cells (Fig. 4 a2). However, mitochondria in cells with irregular shapes showed normal appearances (Fig. 4 a3). Fluorescent imaging of living cells showed that GFP-KDEL-labeled ER was distributed in a reticular pattern throughout the cytoplasm (Fig. 4 b1). Twenty-four hours after ADM treatment, the distribution of ER was highly similar to that of control (Fig. 4 b2, b3). Control cells expressing Golgi-GFP showed perinuclear, tubular Golgi structures (Fig. 4 c1), whereas the Golgi dispersed throughout the cytoplasm with a dot-like pattern after ADM application (Fig. 4 c2, c3). Under normal growth conditions, the expression of Tomato-LC3 was detectable by fluorescence microscopy (Fig. 4 d1), in greater than 90% of the cells. After 24 h of ADM (0.05 μg/ml) treatment, there was a dramatic increase of punctuate vesicular structures labeled with Tomato-LC3. These vesicles were found concentrated at the juxtanuclear region (Fig. 4 d2). Similar things happened in cells with long spines (Fig. 4 d3).

Fig. 4

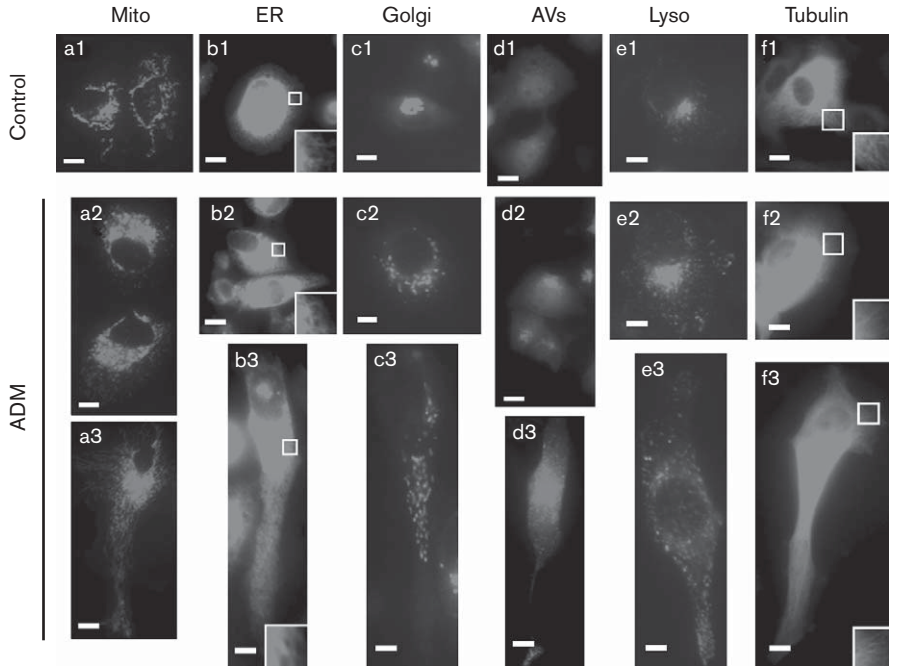

Cellular organelle alterations of human liver-derived hepatoma G2 (HepG2) cells induced by adriamycin (ADM) treatment. HepG2 cells were transfected with DsRed-Mit (Mito), GFP-KDEL (ER), Golgi-GFP (Golgi), Tomato-LC3 (AVs), GFP-Lgp120 (Lyso), GFP-α-tubulin (Tubulin) plasmids, respectively. After 24 h of ADM (0.05 μg/ml) treatment, fluorescent protein-labeled cellular organelles were detected under fluorescence microscopy (Olympus) (a2–f2, a3–f3). Some of the ADM-treated HepG2 cells exhibited a differentiation characteristic with long spines (a3–f3). Cells without ADM treatment were used as control (a1–f1). Scale bars: 10 μm.

Interestingly, there was no significant difference in HepG2 cells at 24 h after the same treatment when cells were transfected with Lgp120 (also known as lysosome-associated membrane glycoprotein 1, a glycoprotein mainly localized to the limiting membranes of lysosomes and late endosomes [11]) fused to GFP (Fig. 4 e1–e3). In addition, microtubules appeared to be intact at 24 h after ADM (0.05 μg/ml) treatment compared with those of control cells (Fig. 4f1–f3).

Induction of autophagy after ADM treatment

On the basis of the observations that enhanced production of LC3-labeled AVs was detected in HepG2 cells after ADM application (Fig. 4 d1–d3), we hypothesize that ADM induced the activation of the autophagic process. As the conversion of soluble LC3-I to lipid bound LC3-II is the most reliable marker for autophagy activation [12], western blotting was performed using an anti-LC3 polyclonal antibody. After ADM (0.05 μg/ml) treatment, the upregulation of LC3-II occurred at 12 h, peaked at 36 h, and then decreased to normal level after 60 h (Fig. 5). Adobe Photoshop software (Adobe, San Jose, California, USA) was used for the quantification of immunoblots. Consistent with earlier results, these data showed that ADM application leads to the induction of autophagy.

Fig. 5

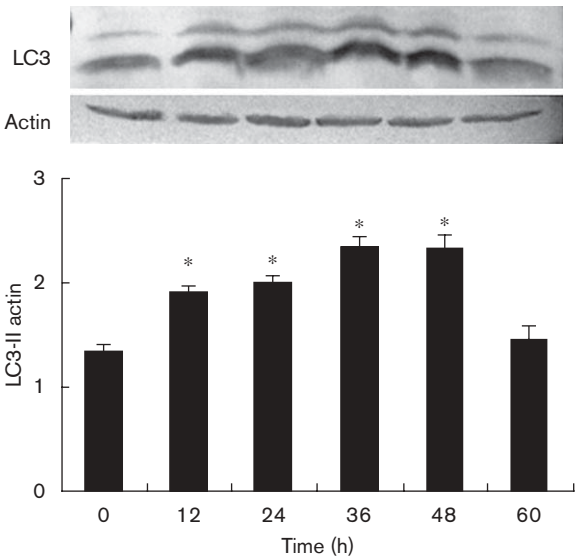

The upregulation of LC3-II occurred upon adriamycin (ADM) treatment. After ADM (0.05 μg/ml) application, human liver-derived hepatoma G2 (HepG2) cells were lysed and analyzed by western blotting using anti-LC3 antibody at the indicated time-points. The amount of LC3-II was quantified relative to the level of actin. Results are representative of three independent experiments. *$P<0.001$ compared with untreated control (0 h).

Discussion

ADM is a commonly used anticancer drug, which causes the initiation of DNA damage and kills tumor cells. Emerging lines of evidence identified the molecular targets of this drug [3], whereas the process leading to killing of the hepatoma cells and drug resistance, particularly in relation to cellular organelles, is poorly known. It will be very important to determine the detailed mechanism of the synergistic effect of the treatment both in developing a novel approach to killing cancer cells and in elucidating a general mechanism of cell death. In this study, HepG2 cells were exposed to different doses of ADM for up to 60 h. ADM exerted a cytotoxic effect during the early stage of incubation, with a dramatic decreased cell proliferation. Thereafter, a gradual increase was observed (Fig. 1a). Moreover, at this time point, some of the HepG2 cells died in response to ADM treatment (Fig. 1b, upper panels, arrowheads), whereas other living cells exhibited a remarkable altered morphology with long spines (asterisks). We further investigated the alterations of cellular organelles at 24 h after ADM treatment.

Mitochondrial dysfunction plays a principal role in apoptotic cell death. It has been reported that ADM induces apoptosis of HepG2 cells with rapid cell shrinkage, increased cell granularity, chromatin condensation, and mitochondrial membrane potential collapse [7]. Our findings showed that after ADM treatment, a large number of the mitochondria were fragmented in dying HepG2 cells. However, mitochondria in remaining living cells showed normal appearances (Fig. 4). On the basis of these findings, we hypothesize that mitochondria may be the direct target of ADM treatment. These results also suggest that impairing mitochondrial function might be an effective way to overcome drug resistance.

Anticancer drugs, including ADM, frequently act by inducing apoptosis of hepatoma cells [13], but recent studies have indicated that apoptosis may not be the primary mechanism of cell death [14–16]. Autophagy, also designed as type II programmed cell death, is a physiological mechanism that involves the sequestration of cytoplasm and intracellular organelles into membrane vacuoles called autophagosomes, and results in their eventual enzymatic degradation [17]. The role of autophagy in cancer cells in response to anticancer therapeutics is still controversial. It has been reported that autophagy protects some cancer cells against anticancer treatment by inhibiting the apoptotic pathway, whereas other cancer cells undergo autophagic cell death after anticancer therapy [18,19]. In this study, HepG2 cells treated with 0.05 μg/ml of ADM for 24 h showed an ultrastructural appearance consistent with the characteristics of autophagy under TEM observation. Confirmatory experiments were performed with plasmid transfection showing that ADM stimulated AVs formation. In addition, the upregulation of LC3-II occurred at 12 h, peaked at 36 h, and then decreased to normal level after 60 h of ADM incubation (Fig. 5), implying that the autophagic process was involved in the early responses to ADM treatment.

It is also intriguing to note that tubular Golgi structures were distributed in perinuclear regions in healthy HepG2 cells (Fig. 4 c1), whereas the Golgi apparatus dispersed throughout the cytoplasm with a dot-like pattern at 24 h after ADM application (Fig. 4 c2, c3). It has been widely accepted that the drug transporter P-gp plays an important role in drug resistance. Tumor cells express a high level of this surface protein. P-gp has been found to be located in the Golgi apparatus in drug-induced resistant cells and in intrinsic resistant cells [9]. As the Golgi apparatus acts as the preferential intracytoplasmic site of drug accumulation in resistant cells, it can sequester ADM away from the nuclear target.

In summary, this study showed that some cellular organelles of HepG2 cells altered their subcellular distribution or morphology after ADM treatment, including mitochondria, AVs, and the Golgi apparatus. Future work is needed to explore the potential relationship of these events, and to understand the mechanisms of cancer cell death and the molecular basis of resistance to ADM.

Acknowledgements

The authors are grateful to T. Johansen for ptdTomato-LC3 plasmid, P. Luzio for GFP-Lgp120, D. Toomre for Golgi-GFP, B. Boyles for GFP-KDEL, and X.J. Cai for helpful suggestions.

References

1 Olweny CL, Toya T, Katongole-Mbidde E, Mugerwa J, Kyalwazi SK, Cohen H. Treatment of hepatocellular carcinoma with adriamycin. *Cancer* 1975; **36**:1250–1257.
2 Otten SL, Stutzman-Engwall KJ, Hutchinson CR. Cloning and expression of daunorubicin biosynthesis genes from Streptomyces peucetius and S. peucetius subsp. caesius. *J Bacteriol* 1990; **172**:3427–3434.
3 Gewirtz DA. A critical evaluation of the mechanisms of action proposed for the antitumor effects of the anthracycline antibiotics adriamycin and daunorubicin. *Biochem Pharmacol* 1999; **57**:727–741.
4 Chang G, Roth CB. Structure of MsbA from E. coli: a homolog of the multidrug resistance ATP binding cassette (ABC) transporters. *Science* 2001; **293**:1793–1800.
5 Lasagna N, Fantappie O, Solazzo M, Morbidelli L, Marchetti S, Cipriani G, *et al.* Hepatocyte growth factor and inducible nitric oxide synthase are involved in multidrug resistance-induced angiogenesis in hepatocellular carcinoma cell lines. *Cancer Res* 2006; **66**:2673–2682.
6 Barraud L, Merle P, Soma E, Lefrancois L, Guerret S, Chevallier M, *et al.* Increase of doxorubicin sensitivity by doxorubicin-loading into nanoparticles for hepatocellular carcinoma cells in vitro and in vivo. *J Hepatol* 2005; **42**:736–743.
7 Ye N, Qin J, Liu X, Shi W, Lin B. Characterizing doxorubicin-induced apoptosis in HepG2 cells using an integrated microfluidic device. *Electrophoresis* 2007; **28**:1146–1153.
8 Kim SJ, Park KM, Kim N, Yeom YI. Doxorubicin prevents endoplasmic reticulum stress-induced apoptosis. *Biochem Biophys Res Commun* 2006; **339**:463–468.

9 Arancia G, Calcabrini A, Meschini S, Molinari A. Intracellular distribution of anthracyclines in drug resistant cells. *Cytotechnology* 1998; **27**:95–111.
10 Yang Y, Fukui K, Koike T, Zheng XX. Induction of autophagy in neurite degeneration of mouse superior cervical ganglion neurons. *Eur J Neurosci* 2007; **26**:2979–2988.
11 Fukuda M. Lysosomal membrane glycoproteins. Structure, biosynthesis, and intracellular trafficking. *J Biol Chem* 1991; **266**:21327–21330.
12 Kabeya Y, Mizushima N, Ueno T, Yamamoto A, Kirisako T, Noda T, *et al*. LC3, a mammalian homologue of yeast Apg8p, is localized in autophagosome membranes after processing. *EMBO J* 2000; **19**:5720–5728.
13 Lee TK, Lau TC, Ng IO. Doxorubicin-induced apoptosis and chemosensitivity in hepatoma cell lines. *Cancer Chemother Pharmacol* 2002; **49**:78–86.
14 Viktorsson K, Lewensohn R, Zhivotovsky B. Apoptotic pathways and therapy resistance in human malignancies. *Adv Cancer Res* 2005; **94**:143–196.
15 Kim R, Emi M, Tanabe K. The role of apoptosis in cancer cell survival and therapeutic overcome. *Cancer Biol Ther* 2006; **5**:1429–1442.
16 Park SS, Kim MA, Eom YW, Choi KS. Bcl-xL blocks high dose doxorubicin-induced apoptosis but not low dose doxorubicin-induced cell death through mitotic catastrophe. *Biochem Biophys Res Commun* 2007; **363**:1044–1049.
17 Reggiori F, Klionsky DJ. Autophagy in the eukaryotic cell. *Eukaryot Cell* 2002; **1**:11–21.
18 Codogno P, Meijer AJ. Autophagy and signaling: their role in cell survival and cell death. *Cell Death Differ* 2005; **12**:1509–1518.
19 Kondo Y, Kanzawa T, Sawaya R, Kondo S. The role of autophagy in cancer development and response to therapy. *Nat Rev Cancer* 2005; **5**:726–734.